Bioorganic Chemistry 57 (2014) 116–120

Contents lists available at ScienceDirect

Bioorganic Chemistry

journal homepage: www.elsevier.com/locate/bioorg

Hydroxamates of *para*-aminobenzoic acid as selective inhibitors of HDAC8

Umasankar Kulandaivelu [a], Laxmi Manasa Chilakamari [a], Surender Singh Jadav [b], Tadikonda Rama Rao [c], K.N. Jayaveera [d], Boyapati Shireesha [a], Alexander-Thomas Hauser [e], Johanna Senger [e], Martin Marek [f], Christophe Romier [f], Manfred Jung [e,*], Venkatesan Jayaprakash [b,g,*]

[a] Medicinal Chemistry Research Division, Vaagdevi College of Pharmacy, Hanamkonda, Warangal 506 001, Andhra Pradesh, India
[b] Department of Pharmaceutical Sciences and Technology, Birla Institute of Technology, Mesra, Ranchi 835 215, Jharkhand, India
[c] Blue Birds College Of Pharmacy, Hanamkonda, Warangal 506 015, Andhra Pradesh, India
[d] Department of Chemistry, Jawaharlal Nehru Technological University Anantapur, College of Engineering, Anantapur 515 002, Andhra Pradesh, India
[e] Institute of Pharmaceutical Sciences, Universität Freiburg, Albertstr. 25, 79104 Freiburg, Germany
[f] Integrated Structural Biology Department, IGBMC, 1 rue Laurent Fries, 67404 Illkirch, France
[g] Valens Pharma Services, Regus Citi Centre, Level 6, Chennai Citi Centre, 10/11, Dr. Radhakrishnan Salai, Chennai 600 004, Tamil Nadu, India

ARTICLE INFO

Article history:
Received 2 May 2014
Available online 3 September 2014

Keywords:
p-Aminobenzoic acid derivatives
Hydroxamates
HDAC8
Inhibitors
Molecular docking

ABSTRACT

A series of hydroxamates (**4a–4l**) were prepared from *p*-aminobenzoic acid to inhibit HDAC8. The idea is to substitute rigid aromatic ring in place of less rigid piperazine ring of hydroxamates reported earlier by our group. It is expected to increase potency retaining the selectivity. Result obtained suggested that the modifications carried out retained the selectivity towards HDAC8 isoform and increasing the potency in very few cases. Increase in potency is also associated with variation in cap aryl region. Two compounds (**4f** & **4l**) were found to inhibit HDAC8 at concentrations (IC_{50}) less than 20 μM.

1. Introduction

HDACs are validated targets for anticancer therapy and two inhibitors, Vorinostat (2006) [1] and Romidepsin (2009), have already been approved for cancer therapy. Another 10–20 HDAC inhibitors are now currently in various phase of clinical trails [2,3]. Side-effects reported with approved drugs in market and that are in clinical trials are due to nonspecific (class) and nonselective (isoform) inhibition of HDAC [3]. Hence efforts are being continually made to develop isoform-specific inhibitors against cancer relevant targets.

Class I specific inhibitors with isoform selective inhibition of HDAC1/2 has been achieved and structural requirement for HDAC1/2 inhibition has been established to a greater extent [4–8]. Isoform selective inhibitors against HDAC8 are very interesting due to their potential application in Neuroblastoma [9] and inflammatory conditions [10]. Till date very few selective inhibitors of HDAC8 were reported [11–15].

Our group has already reported selective HDAC8 inhibitors with piperazine linkers [11,12]. They are selective towards HDAC8 isoform but potency is in the range of 33–43 μM. Uesato et al. have shown that more rigid aromatic rings in place of alicyclic rings increases the potency of the HDAC inhibitors using partially purified HDAC from human T cell leukemia Jurkat cell [16]. In an attempt to increase the potency, the current study explores hydroxamates of para-aminobenzoic acid (PABA)-replacing piperazine with PABA as an aromatic equivalent.

2. Results and discussion

2.1. Chemistry

A small library of twelve (**4a**–**4l**) PABA-derived hydroxamates was synthesized following the reaction outlined in Scheme 1 [17]. Methyl hydrazine carbodithioate (1) was synthesized according to procedure reported by Klayman et al. [18] Schiff's bases of compound 1 with corresponding aromatic aldehydes and ketones provided compounds **2a**–**2l** in the presence of catalytic amount of sulfuric acid in methanol under reflux for about 6–7 h. Refluxing

* Corresponding authors. Address: Department of Pharmaceutical Sciences and Technology, Birla Institute of Technology, Mesra, Ranchi 835 215, Jharkhand, India (V. Jayaprakash).
E-mail addresses: manfred.jung@pharmazie.uni-freiburg.de (M. Jung), drvenkatesanj@gmail.com (V. Jayaprakash).

http://dx.doi.org/10.1016/j.bioorg.2014.08.005
0045-2068/

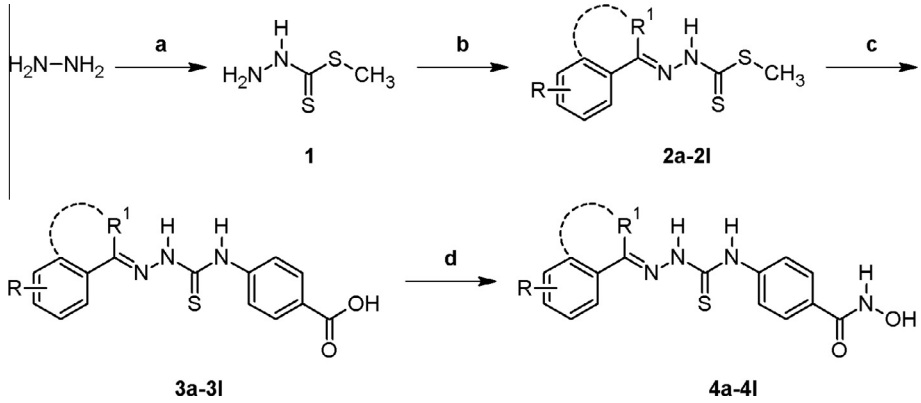

Scheme 1. Reagents and conditions: (a) KOH/*i*-PrOH, CS_2, stirring <10 °C, 2.5 h; CH_3I, stirring, <10 °C, 3.5 h; (b) R–C_6H_4–CO–R^1/Isatin, MeOH, H_2SO_4 [cat], reflux, 6–7 h; (c) *p*-aminobenzoic acid/EtOH, reflux, 3–4 days and (d) i. C_6H_5OCOCl, $(Et)_3NH$, THF, NH_2OH, stirring, rt, 4 h.

compound **2a**–**2l** with PABA in ethanol till the completion of evolution of methyl mercaptan (3–4 days) provided corresponding acids **3a**–**3l**. The acids **3a**–**3l** were then treated with phenylchloroformate in the presence of triethylamine in tetrahydrofuran. The resulting anhydride upon reaction with hydroxylamine produced desired hydroxamates **4a**–**4l**.

The final hydroxamate derivatives **4a–4l** were characterized by their ^{1}H NMR and ES-MS spectral data. All the hydroxamate derivatives (**4a**–**4l**) showed a characteristic peak for the hydroxamate –OH proton between δ 2.0 and 2.4 ppm as broad singlet, aldehydic –CH proton between δ 8.0 and 8.4 ppm as a singlet, ketonic –CH_3 proton between δ 1.6 and 1.8 ppm as a singlet and the methyl –CH_3 between 2.5 and 2.9 as a singlet. The structure, physico-chemical and spectral characterization of compounds **4a**–**4l** were presented.

2.2. Anti-HDAC screening assay

All the twelve compounds (**4a**–**4l**) were tested for their inhibitory activity against class 1 HDAC (HDAC1 and HDAC8) and a class 2 HDAC (HDAC6). This is to test the class selectivity and isoform specificity. For this purpose, we used a homogeneous fluorescent assay [19,20]. PCI34051, a selective inhibitor of HDAC8 has been used as a standard for comparison [21]. Human HDAC8 was produced using a protocol adapted from method reported by Vannini et al. [22]. Percentage inhibition of HDAC1, 6 and 8 were measured at 50 and 100 μM respectively. The compounds exhibited good results against HDAC8 and a clear indication of class 1 selectivity and HDAC8 specificity within class 1 (Table 1). All the twelve compounds inhibited HDAC8. Two compounds (**4f**-IC_{50} 19.7 ± 0.9 μM & **4k**-IC_{50} 15.7 ± 1.0 μM) were found to inhibit HDAC8 at a concentration below 20 μM. While another two compounds (**4a**-IC_{50} 27.6 ± 2.7 and **4k**-IC_{50} 23.3 ± 1.6) between 20 μM and 30 μM and three compounds (**4b**-IC_{50} 38.7 ± 4.9 μM; **4d**-IC_{50} 46.3 ± 5.1 μM and **4i**-IC_{50} 38.1 ± 4.1 μM) between 30 μM and 50 μM. Between 50 μM and 100 μM three compounds (**4c**-IC_{50} 93.5 ± 10.2 μM; **4h**-IC_{50} 80.5 ± 3.6 μM and **4j**-IC_{50} 53.6 ± 3.9 μM) exhibited inhibition while the rest showed inhibition only above 100 μM.

Compound **4a**, **4h** and **4k** differ in R1 substitution. It seems the bulkier phenyl ring (**4k**) is favorable at R1 position followed by –H and then by –CH_3. Incase of benzaldehyde hydrazones (**4a**–**4e** & **4g**), an unsubstituted aryl head was found to be favorable as substitution (at least all substitutions in this library) leads to decreased activity except Fluoro derivative (**4f**). In case of acetophenone hydrazones (**4h**–**4j**), the compound with an unsubstituted cap group (**4h**) was found to be less potent when compared with substituted counterparts (**4i**–**4j**). Compounds **4e** and **4i** vary only at R1 substitution, compound **4i** was found to be 4-fold potent than compound **4e**. It is understood that R1 methyl group has the ability to influence activity with respect to change in substitution of cap aryl region. But this fact should be tested with analogs of **4i** having variation at cap aryl region. The most potent one in this series is compound **4l**, which is a cyclic ketone.

Compounds **4b**, **4e** and **4l** resembled the piperazine derivatives reported earlier (**5a**, **5b** and **5c**, Fig. 1). Only in case of **4l** presence of an aromatic ring in the linker portion made the molecule active and potent when compared with its piperazine counterpart **5a** (not active). In case of the 2-hydroxy derivatives (**4b** and **5a**: IC_{50} 33.67 μM) they were found to be active at almost equal concentrations. While in case of 4-chloro derivatives (**4e** and **5b**: IC_{50} 43.16 μM), the piperazine derivative performed better than its PABA counterpart. The comparison reveals that rigidity of the linker alone will not make a molecule potent, instead it may play a major role in enhancing potency when its length is optimal and has a cap region with appropriate size and functional groups.

2.3. Binding mode analysis

Molecular docking analysis (**GLIDE 5.0**) was carried out to understand the crucial interaction of **4f** and **4l** (Fig. 2). Both are showing similar binding mode near the Zn^{2+} ion. Carbonyl O of hydroxamate interacts with Zn^{2+} while hydroxyl O of hydroxamate did not show any interaction with Zn^{2+}. An unusual H-bonding interaction was observed between hydroxamate NH with backbone carbonyl O of GLY151. The aromatic ring of PABA established π–π interaction with HIS143 & PHE152. The cap region is largely exposed to solvent, while the NH–CS–NH–N = portion interacts with the hydrophobic residues in the periphery (ASP101, MET274, PHE207, PHE208, GLY206). The compounds **4i** and **4k** also exhibited similar binding pattern.

All the other compounds exhibited usual binding pattern of hydroxamate functional group with Zn^{2+}, 3 H-bonding interactions (1. hydroxamate carbonyl O with Hydroxyl H of TYR306, 2. hydroxamate hydroxyl H with backbone carbonyl O of HIS142 and 3. hydroxamate amido H with backbone carbonyl O of HIS143) and π–π interaction of aryl group of PABA with HIS180 (Fig. 2). These facts once again establish that the cap region definitely plays a role in increasing the potency and even an unusual binding mode is also possible with few potent molecules.

3. Experimental

3.1. General

Melting points were determined using Thermonik Melting Point Apparatus (Campbell Electronics, India) by capillary method and

Table 1
HDAC inhibitory activity of compounds **4a–4l**.

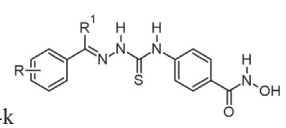

4a-4k

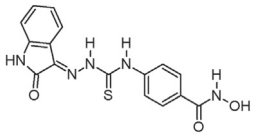

4l

Code	R	R1	hHDAC1 (% Inhibition @ 50 μM)	hHDAC6 (% Inhibition @ 100 μM)	hHDAC8 (IC_{50} in μM)[b]
4a	–H	–H	21.5	30	27.6 ± 2.7
4b	2-OH	–H	32.4	13	38.7 ± 4.9
4c	4-OCH_3	–H	24.7	19	93.5 ± 10.2
4d	–$N(CH_3)_2$	–H	<10	20	46.3 ± 5.1
4e	4-Cl	–H	<10	41	133.5 ± 18.4
4f	4-F	–H	<10	23	19.7 ± 0.9
4g	4-NO_2	–H	<10	29	323.5 ± 38.0
4h	–H	–CH_3	<10[a]	18	80.5 ± 3.6
4i	4-Cl	–CH_3	17.6[a]	33	38.1 ± 4.1
4j	3-NO2	–CH_3	30.7[a]	48	53.6 ± 3.9
4k	–H	–C_6H_5	45.9	44	23.3 ± 1.6
4l	–isatin–		<10[a]	41	15.7 ± 1.0
PCI34051			48.3[a]	41	26 ± 8 (in nM)

[a] % Inhibition @ 100 μM.
[b] Mean ± SEM of three different experiments.

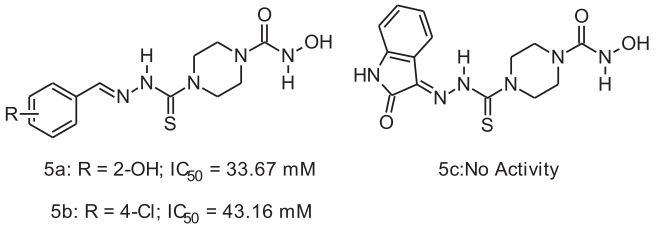

Fig. 1. Selective HDAC inhibitors with piperazine linkers reported earlier.

are uncorrected. ^{1}H NMR spectra were recorded at 400 MHz in DMSO-d_6 using a Bruker Avance 400 instrument (Bruker Instruments Inc., USA). Chemical shifts δ were measured in ppm units relative to tetramethylsilane (TMS). Fast-atom bombardment (FAB) mass spectra were recorded on a Jeol SX 102/DA-6000 mass spectrometer (Jeol Ltd. Akishima, Tokyo, Japan) using argon/xenon (6 kV, 10 mA) as FAB gas, *m*-nitrobenzyl alcohol as matrix, and 10 kV as accelerating voltage at room temperature. Elemental analysis was performed on a Vario EL III Elemental Analyser (Elementar, Germany) using sulfanilamide as standard. All chemicals were purchased from Merck, Spectrochem or CDH, India. Solvents were of reagent grade and were purified and dried by standard procedure. Reactions were monitored by thin-layer chromatography on silica gel plates in either iodine or UV chambers. Intermediates were characterized by IR spectroscopic analysis and elemental analysis for CHNS. In the elemental analysis, the observed values were within ±0.4% of the calculated values. Final compounds were characterized by ^{1}H NMR and FAB-MS. The final yields and the physicochemical and spectral data of final compounds **4a–4l** are presented.

*3.1.1. General synthesis of methyl hydrazinecarbodithioate (**1**)*

To a cooled solution of potassium hydroxide (0.1 M, 6.6 g/7 mL) was added 2-propanol (7 mL) hydrazine hydrate (85% solution, 0.1 M, 6 mL) with stirring. Ice-cooled carbondisulfide (0.1 M, 10 mL) was added drop wise to the above stirred solution that was maintained <10 °C over 1.5 h. The bright yellow mixture obtained was further stirred for 1 h and then ice-cooled iodomethane (0.1 M, 7 mL) was added drop wise over a period of 2 h. Stirring was continued for an additional 1.5 h to obtain a white precipitate of **1**. Filtered, washed with ice-cooled water and recrystallized from dichloromethane.

*3.1.2. General synthesis of Schiff bases methylhydrazine carbodithioate (**2a–2l**)*

Methyl hydrazinecarbodithioate **1** (0.01 M, 1.22 g) and (un)substituted aromatic aldehydes/ketone (0.012 M) were dissolved in methanol. To this mixture catalytic amount of concentrated sulfuric acid was added and refluxed for 6–7 h. The reaction mixture turned yellow as the methylhydrazine carbodithioate dissolved and the yellow product began to precipitate. The solid obtained was filtered, dried and recrystallized from suitable solvent.

*3.1.3. General synthesis of 4-[(2-arylidenehydrazyl)-carbothionyl]-aminobenzoic acid (**3a–3l**)*

PABA (0.005 M, 0.685 g) was added to appropriate Schiff base (**2a–2l**, 0.005 M) in ethanol (25 mL) and refluxed until the evolution of methyl mercaptan almost completely ceased. Solvent present in the reaction mixture was evaporated under vacuum and the solid was collected and washed with cold ethanol, further purified by recrystallization from suitable solvent.

*3.1.4. General synthesis of N-hydroxy-4-[(2-arylidenehydrazinyl)-carbothionyl]-aminobenzamide (**4a–4l**)*

Phenyl chloroformate (0.001 M) and triethylamine (0.001 M) were added to an ice-cooled solution of appropriate benzoic acid derivative (**3a–3l**, 0.001 M) in dry THF and the mixture was stirred for 1 h. The solid obtained was filtered off and to the filtrate was added freshly prepared solution of hydroxylamine. After stirring at room temperature for 3 h, the solid obtained was filtered, dried and recrystallized from suitable solvent.

3.2. Anti-HDAC screening assay

The HDAC 1 assay was carried out in 96-well plates with a reaction volume of 60 μL, containing the fluorescent HDAC substrate MAL (10.5 μM), HDAC (10 μL) and the inhibitors in DMSO in varying concentrations (3 μL). The tests for HDAC 8 activity were performed in 96-well half-area plates with a reaction volume of 30 μL. Here, ZMTFAL, a fluorogenic substrate bearing a trifluoroacetyl group was used (10.5 μM). After 90 min of incubation, in both assays the deacetylation reaction was stopped by the addition of the endopeptidase trypsin. The deacetylated metabolites (ML or

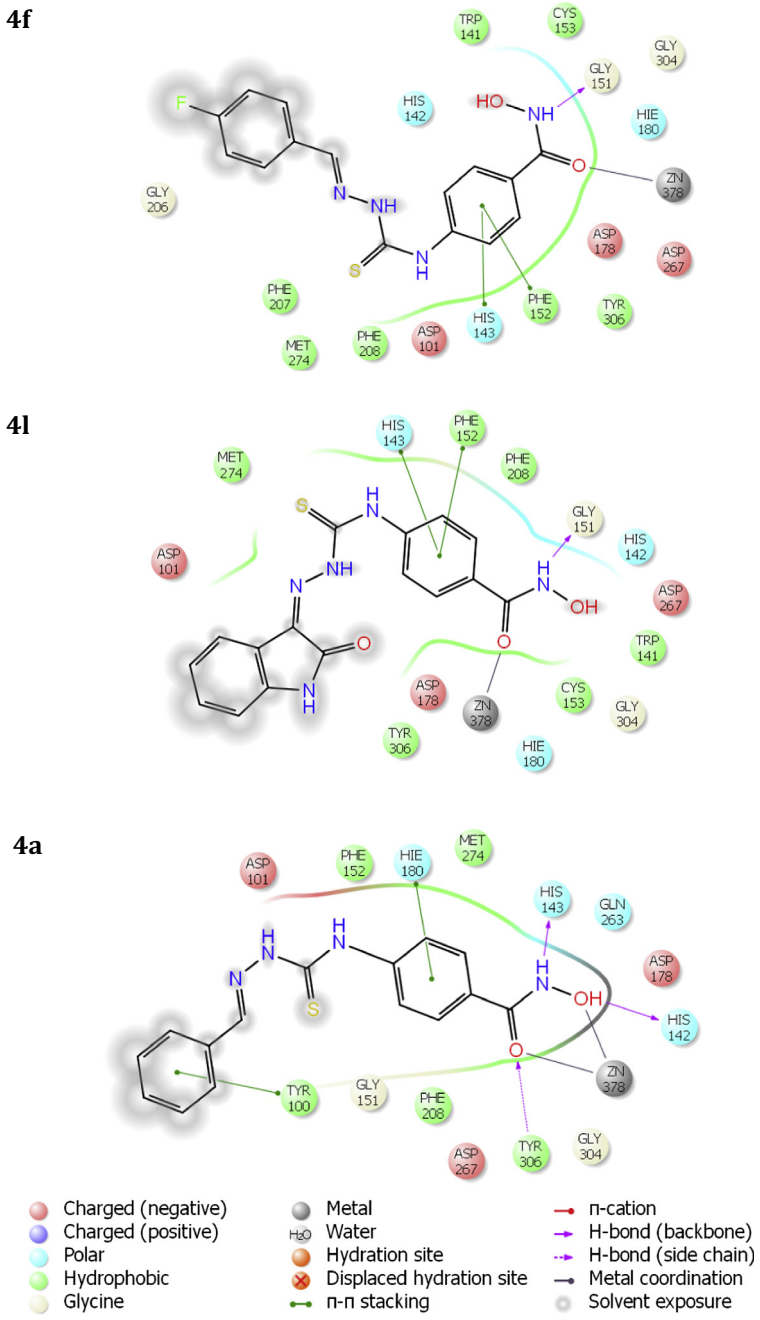

Fig. 2. 2D-plot of complex of **4f**, **4l** and **4a** with HDAC8.

ZML) were digested by trypsin in order to form a fluorophore with an emission maximum that differs from the that of the original substrate. The fluorescence was measured in a plate reader (BMG Polarstar) with a coumarin filter (excitation 390 nm and emission 460 nm). The amount of remaining substrate in the positive control with inhibitor versus negative control without inhibitor was employed to calculate inhibition. All determinations were carried out in duplicate [21].

3.3. Docking studies

3.3.1. Materials and methods

All computational analysis was carried out on a Red Hat 5.0 Linux platform running on a Dell Precision work station with Intel core 2 quad processor and 8 GB of RAM.

3.3.2. Molecular docking protocol

The X-ray crystallographic structure of human HDAC8 complexed with SAHA (PDB: 1T69) with resolution 2.91 Å; *R*-value 0.249 (observed) was acquired from protein data bank (http://www.pdb.org/pdb/explore/explore.do?structureId=1T69). It contains single chain; the protein preparation wizard (Maestro, version 8.5, Schrodinger, LLC, 2008) was employed to refine the protein structure. Bond orders were assigned, hydrogens were added and water molecules were deleted. Metals were treated; it contains the Zinc ion (Zn^{2+}). Heterostate for co-crystallized ligand was generated using Epik and Hydrogen bond of protein was allocated using Protassign. The energy minimization of protein was exerted by impref minimization at pH 7.0 and OPLS-2005 force field. The receptor grid was generated around the reference/bound ligand SAHA (Octanedioic Acid Hydroxyamide Phenylamide) with

default parameters using GLIDE5.0 which was implemented in Schrodingers LLC; was also employed for the automated flexible molecular docking protocol. All the 3-dimentional structures of ligands were drawn using Maestro, prepared by ligprep, output were docked in the HDAC8 active site. The extra precisions docking (XP) was employed for the current docking study and are scored; the ligand receptor interactions were then carried out.

Acknowledgments

The author acknowledge Viswambhara Educational Society, Warangal, AP, India for providing the research facilities and IICT, Hyderabad, AP, India for providing spectral characterization. M.J. and C.R. acknowledge funding from the European Community grant SEtTReND (FP7-Health contract no. 241865) and DFG (Ju295/10-2, within CRU201) and Deutsche Forschungsmeinschaft (DFG: Ju295/13-1)

References

[1] S. Grant, C. Easley, P. Kirkpatrick, Nat. Rev. Drug Discov. 6 (1) (2007) 21–22.
[2] J. Tan, S. Cang, Y. Ma, R.L. Petrillo, D. Liu, J. Hematol. Oncol. 3 (2010) 5.
[3] J.M. Wagner, B. Hackanson, M. Lübbert, M. Jung, Clin. Epigenetics 1 (3) (2010) 117–136.
[4] A.V. Bieliauskas, M.K. Pflum, Chem. Soc. Rev. 37 (7) (2008) 1402–1413.
[5] D.C. Drummond, C.O. Noble, D.B. Kirpotin, Z. Guo, G.K. Scott, C.C. Benz, Annu. Rev. Pharmacol. Toxicol. 45 (2005) 495–528.
[6] Y. Itoh, T. Suzuki, N. Miyata, Curr. Pharm. Des. 14 (6) (2008) 529–544.
[7] N. Khan, M. Jeffers, S. Kumar, C. Hackett, F. Boldog, N. Khramtsov, X. Qian, E. Mills, S.C. Berghs, N. Carey, P.W. Finn, L.S. Collins, A. Tumber, J.W. Ritchie, P.B. Jensen, H.S. Lichenstein, M. Sehested, Biochem. J. 409 (2) (2008) 581–589.
[8] T. Suzuki, Chem. Pharm. Bull. (Tokyo) 57 (9) (2009) 897–906.
[9] J.J. Buggy, S. Balasubramanian, Google Patents, 2010.
[10] J. Buggy, S. Balasubramanian, S. Steggerda, WO Patent 2,008,061,160, 2008.
[11] S. Chakrabarty, Jasmine, C. Bhadaliya, B.N. Sinha, A. Mahesh, H. Bai, S.Y. Blond, V. Jayaprakash, Arch. Pharm. (Weinheim) 343 (3) (2010) 167–172.
[12] B. Chetan, M. Bunha, M. Jagrat, B.N. Sinha, P. Saiko, G. Graser, T. Szekeres, G. Raman, P. Rajendran, D. Moorthy, A. Basu, V. Jayaprakash, Bioorg. Med. Chem. Lett. 20 (13) (2010) 3906–3910.
[13] P. Galletti, A. Quintavalla, C. Ventrici, G. Giannini, W. Cabri, S. Penco, G. Gallo, S. Vincenti, D. Giacomini, ChemMedChem 4 (12) (2009) 1991–2001.
[14] K. KrennHrubec, B.L. Marshall, M. Hedglin, E. Verdin, S.M. Ulrich, Bioorg. Med. Chem. Lett. 17 (10) (2007) 2874–2878.
[15] W. Tang, T. Luo, E.F. Greenberg, J.E. Bradner, S.L. Schreiber, Bioorg. Med. Chem. Lett. 21 (9) (2011) 2601–2605.
[16] S. Uesato, M. Kitagawa, Y. Nagaoka, T. Maeda, H. Kuwajima, T. Yamori, Bioorg. Med. Chem. Lett. 12 (10) (2002) 1347–1349.
[17] U. Kulandaivelu, V.G. Padmini, K. Suneetha, B. Shireesha, J.V. Vidyasagar, T.R. Rao, J.K.N.A. Basu, V. Jayaprakash, Arch. Pharm. (Weinheim) 344 (2) (2011) 84–90.
[18] D.L. Klayman, J.F. Bartosevich, T.S. Griffin, C.J. Mason, J.P. Scovill, J. Med. Chem. 22 (7) (1979) 855–862.
[19] B. Heltweg, F. Dequiedt, B.L. Marshall, C. Brauch, M. Yoshida, N. Nishino, E. Verdin, M. Jung, J. Med. Chem. 47 (21) (2004) 5235–5243.
[20] B. Heltweg, M. Jung, J. Biomol. Screening 8 (1) (2003) 89–95.
[21] S. Doubrovinskaia, Rational design, synthesis and evaluation towards a specific histone deacetylase inhibitor for Schistosoma mansoni, University of Freiburg, 2014.
[22] A. Vannini, C. Volpari, P. Gallinari, P. Jones, M. Mattu, A. Carfí, R. De Francesco, C. Steinkühler, S. Di Marco, EMBO Reports 8 (9) (2007) 879–884.